SUPPORTING INFORMATION

Design, Manufacturing and Testing of a Green Non-Isocyanate Polyurethane Prosthetic Heart Valve

Sofia F. Melo[a]*, Alicia Nondonfaz*[a]*, Abdelhafid Aqil*[b]*, Anna Pierrard*[b]*, Alexia Hulin*[a]*, Céline Delierneux*[a]*, Bartosz Ditkowski*[a]*, Maxime Gustin*[a]*, Maxime Legrand*[c]*, Bibian M. E. Tullemans*[d]*, Sanne L. N. Brouns*[d]*, Alain Nchimi*[a]*, Raoul Carrus*[c]*, Astrid Dejosé*[c]*, Johan W. M. Heemskerk*[d]*, Marijke J. E. Kuijpers*[d]*, Jan Ritter*[e]*, Ulrich Steinseifer*[e]*, Johanna C. Clauser*[e]*, Christine Jérôme*[b]*, Patrizio Lancellotti*[a,‡]*, Cécile Oury*[a,‡,*]*

[a] Laboratory of Cardiology, GIGA-Cardiovascular Sciences, University of Liège, Avenue de l'Hôpital 11, B34, 4000 Liège, Belgium.

[b] Center for Education and Research on Macromolecules (CERM), CESAM Research Unit, Department of Chemistry, University of Liège, Allée du 6 août 13, B6a, 4000 Liège, Belgium.

[c] Sirris, Liège Science Park, Rue du Bois Saint-Jean 12, 4102 Seraing, Belgium.

[d] Cardiovascular Research Institute Maastricht (CARIM), Department of Biochemistry, Maastricht University, Universiteitssingel 50, 6200 MD Maastricht, The Netherlands.

[e] Department of Cardiovascular Engineering, Institute of Applied Medical Engineering, Medical Faculty RWTH Aachen University, Pauwelsstraße 20, 52074 Aachen, Germany.

[‡] Authors contributed equally to this work.

[*] Corresponding author: cecile.oury@uliege.be

MATERIALS

Poly(propylene glycol) diglycidyl ether (PPG DE, 380 g/mol) (Sigma-Aldrich), CO_2 (N27) (Air Liquide), tetrabutylammonium iodide (TBAI) (Sigma-Aldrich), poly(tetrahydrofuran) (PTHF, 650 g/mol) (Sigma-Aldrich), toluene anhydrous (Sigma-Aldrich), sodium hydride (Sigma-Aldrich), epichlorohydrin (Sigma-Aldrich), tetrabutylammonium bromide (TBAB) (Sigma-Aldrich), 4,4'-methylenebis(cyclohexylamine) (MBCHA) (Sigma-Aldrich), tris(2-aminoethyl)amine (TAEA) (Merck), chloroform ($CDCl_3$) (VWR Chemicals), deuterated chloroform (Eurisotop), phosphate buffered saline (PBS) (Gibco, Thermo Fisher Scientific), lactate dehydrogenase (LDH) activity assay kit (Sigma-Aldrich), bovine serum albumin (BSA) (Thermo Fisher Scientific), 3,3'-dihexyloxacarbocyanine iodide (Merck), D-phenylalanyl-L-prolyl-L-arginine chloromethyl ketone (PPACK) (Sigma-Aldrich), CRYOcheck™ pooled normal plasma (Cryopep), 5-CLOT NaPTT reagent (NODIA), $CaCl_2$ solution 1M (Merck), Dulbecco's modified Eagle's medium (DMEM) (Gibco, Thermo Fisher Scientific), fetal bovine serum (FBS) (Gibco, Thermo Fisher Scientific), non-essential amino acids (NEAA) (Gibco, Thermo Fisher Scientific), amphotericin B (Gibco, Thermo Fisher Scientific), penicillin/streptomycin (Pen/Strep) (Biowest), trypsin-EDTA solution (Gibco, Thermo Fisher Scientific), 10-oxido-7-oxophenoxazin-10-ium-3-olate (resazurin) (Stemcell Technologies), triton™ X-100 (Merck), paraformaldehyde (PFA) (Merck), phalloidin-Alexa Fluor® 488 (Molecular Probes), 6-diamidino-2-phenylindole dihydrochloride (DAPI) (Merck).

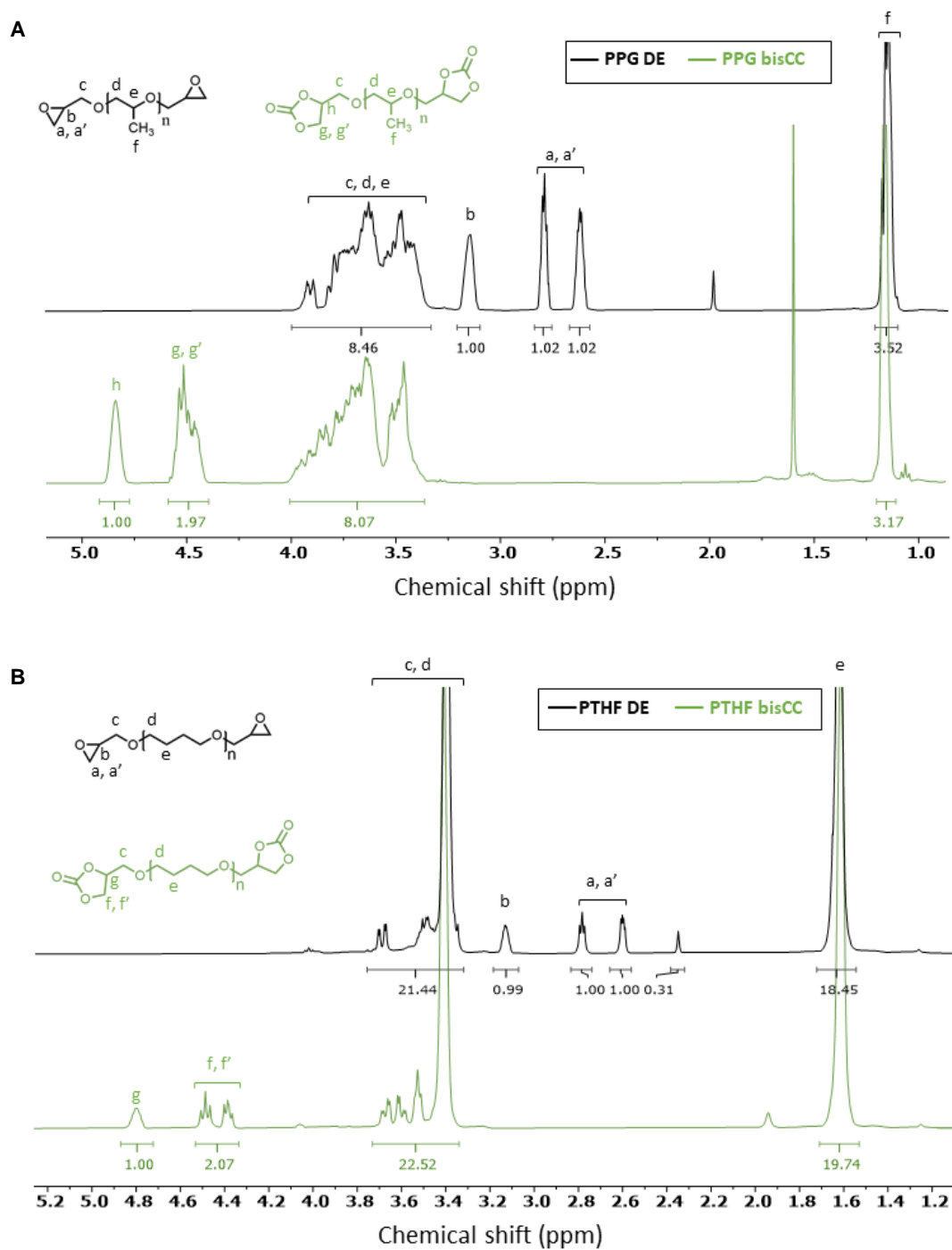**Figure S1. ^{1}H-NMR spectra of synthesized polymers.** A) ^{1}H-NMR spectra of PPG DE and PPG bisCC in deuterated chloroform; B) ^{1}H-NMR spectra of PTHF DE and PTHF bisCC in deuterated chloroform.
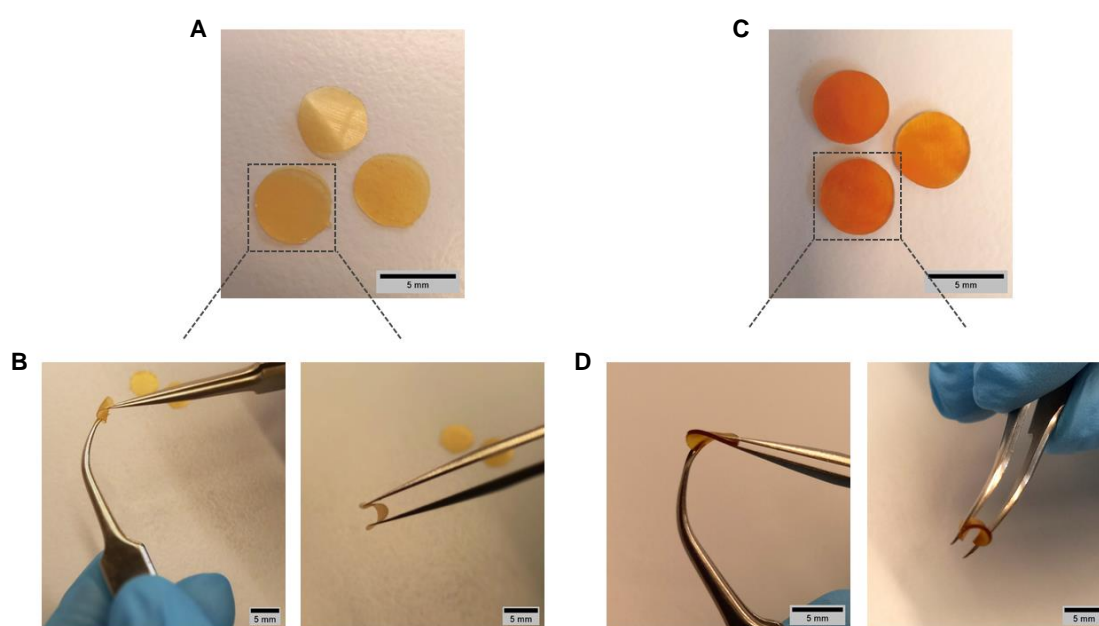
Figure S2. Characteristics of the synthesized NIPU networks. A) Top view of 5-mm discs of PPG-NIPU; B) details of PPG-NIPU flexibility; C) top view of 5-mm discs of PTHF-NIPU; D) details of PTHF-NIPU flexibility.
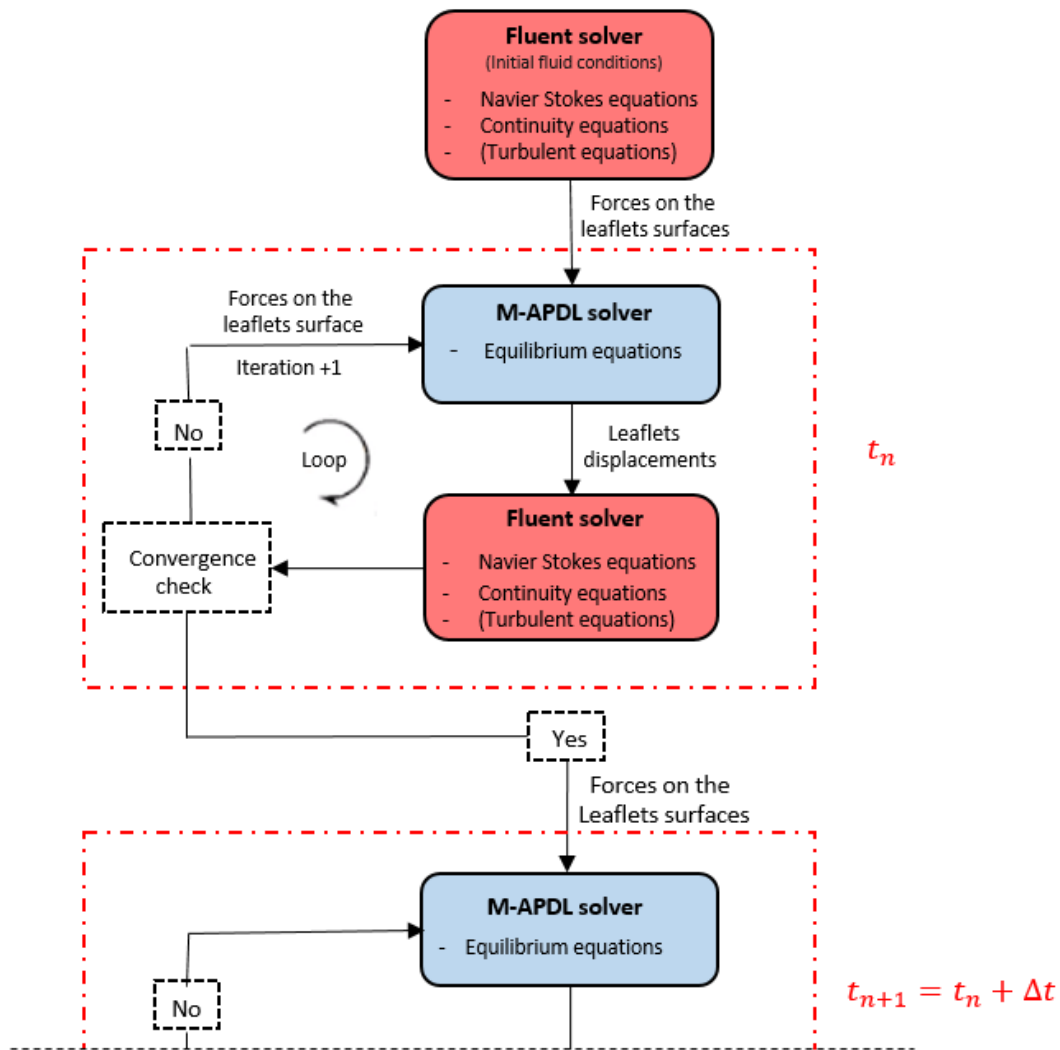
Fluent solver
(Initial fluid conditions)
- Navier Stokes equations
- Continuity equations
- (Turbulent equations)

Forces on the leaflets surfaces

Forces on the leaflets surface

Iteration +1

M-APDL solver
- Equilibrium equations

Loop

No

Leaflets displacements

t_n

Convergence check

Fluent solver
- Navier Stokes equations
- Continuity equations
- (Turbulent equations)

Yes

Forces on the Leaflets surfaces

M-APDL solver
- Equilibrium equations

$t_{n+1} = t_n + \Delta t$

No

Figure S3. Description of the adopted coupling approach. Total analysis time is divided into finite time steps. Within each time step, multiple coupling iterations are performed until the Navier Stokes and Continuity equations governing blood flow (solved in FLUENT solver), leaflet deformation equations (solved in M-APDL solver) and the coupling data transfer have converged. First data transfer is the force data from FLUENT to M-APDL for the specific time step. Using this information, the equations concerning the deformation of the leaflets are solved for this time step. Second data transfer is the leaflet displacement data transferred from M-APDL to FLUENT. With the new position of the leaflet, the fluid equations are solved. Depending on whether the solvers convergence is achieved or not, one can pass to the next time step or perform a new iteration (new loop).
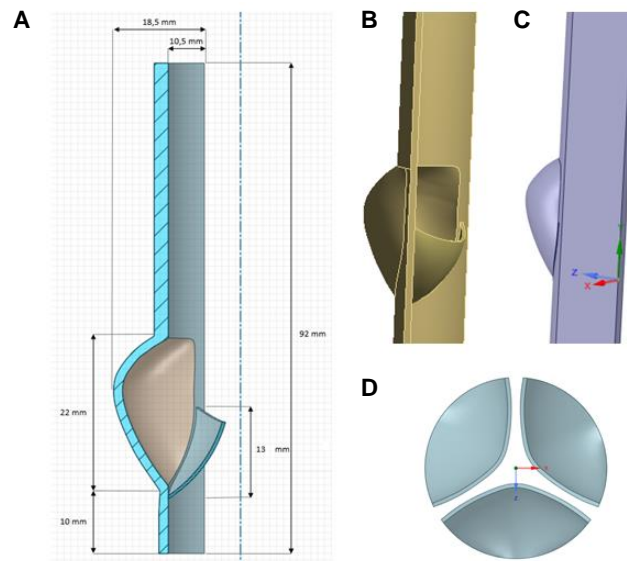
Figure S4. Model geometry. A) longitudinal middle section (the dimensions of this geometrical model refer to a 21-mm diameter valve); B) structure field; C) flow field; D) top view of the three leaflets at the starting point of the simulation.
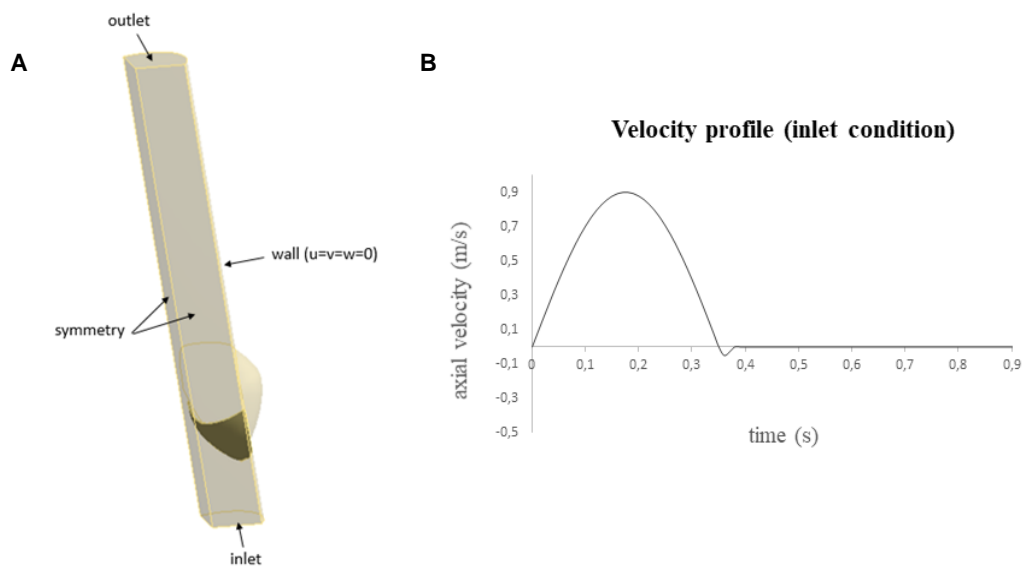

Figure S5. Domains and boundary conditions. A) Structural and fluid domain with the inlet, outlet, symmetry walls and external wall. The ventricular side is defined as the inlet, while the aortic side forms the outlet (the aortic root was removed for clarity); B) inlet transient velocity boundary condition. The cardiac cycle lasts 0.9 s and can be divided in two phases: a systolic phase (0 to 0.35 s) and a diastolic phase (0.35 to 0.9 s).
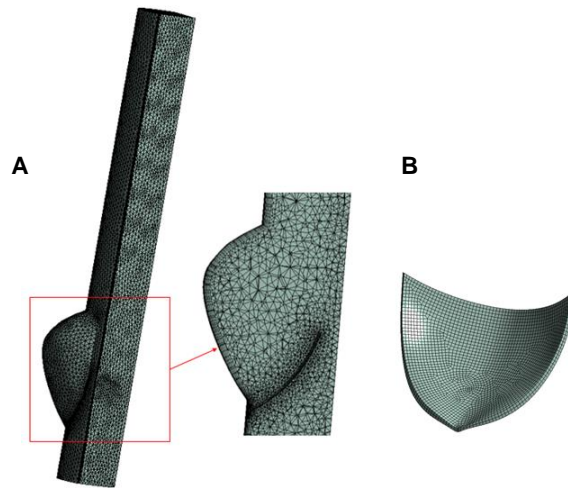
Figure S6. Spatial discretization – meshing. A) Fluid mesh: zoom in a longitudinal section of the fluid domain showing higher mesh density in the vicinity of the leaflet and the wall. Arbitrary Lagrangian-Eulerian (ALE) approach was used to simulate the moving leaflet, meaning that the numerical fluid mesh follows the motion and deformations of the structure; B) leaflet mesh.
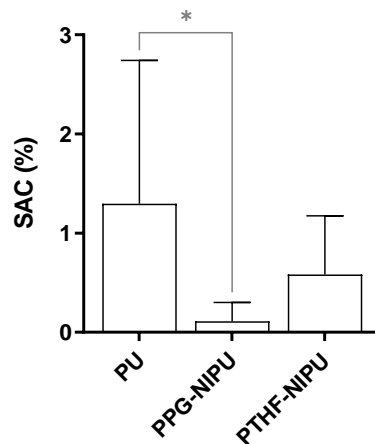

Figure S7. Platelet adhesion measured by surface area coverage (SAC) in PU/NIPU microspots. Data are presented as mean with SD (n = 7). Statistically significant differences between PU and NIPUs were computed using one-way ANOVA (*: adjusted p value ≤ 0.05).
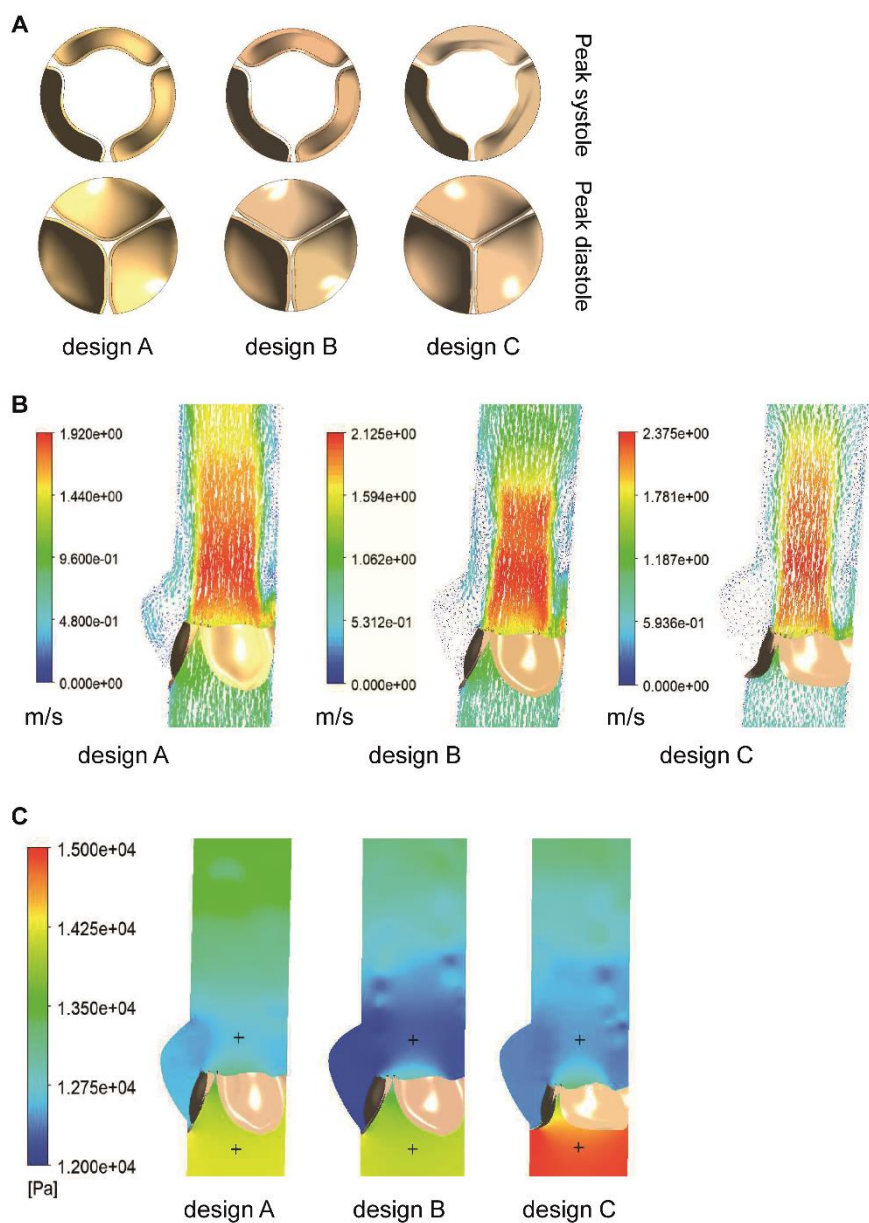
Figure S8. Comparison between different valve designs. A) Open and closed configuration of the leaflets for the designs A, B and C; B) comparison between the velocity vectors at peak systole for the designs A, B and C; C) comparison between the pressure gradients at peak systole for the designs A, B and C.
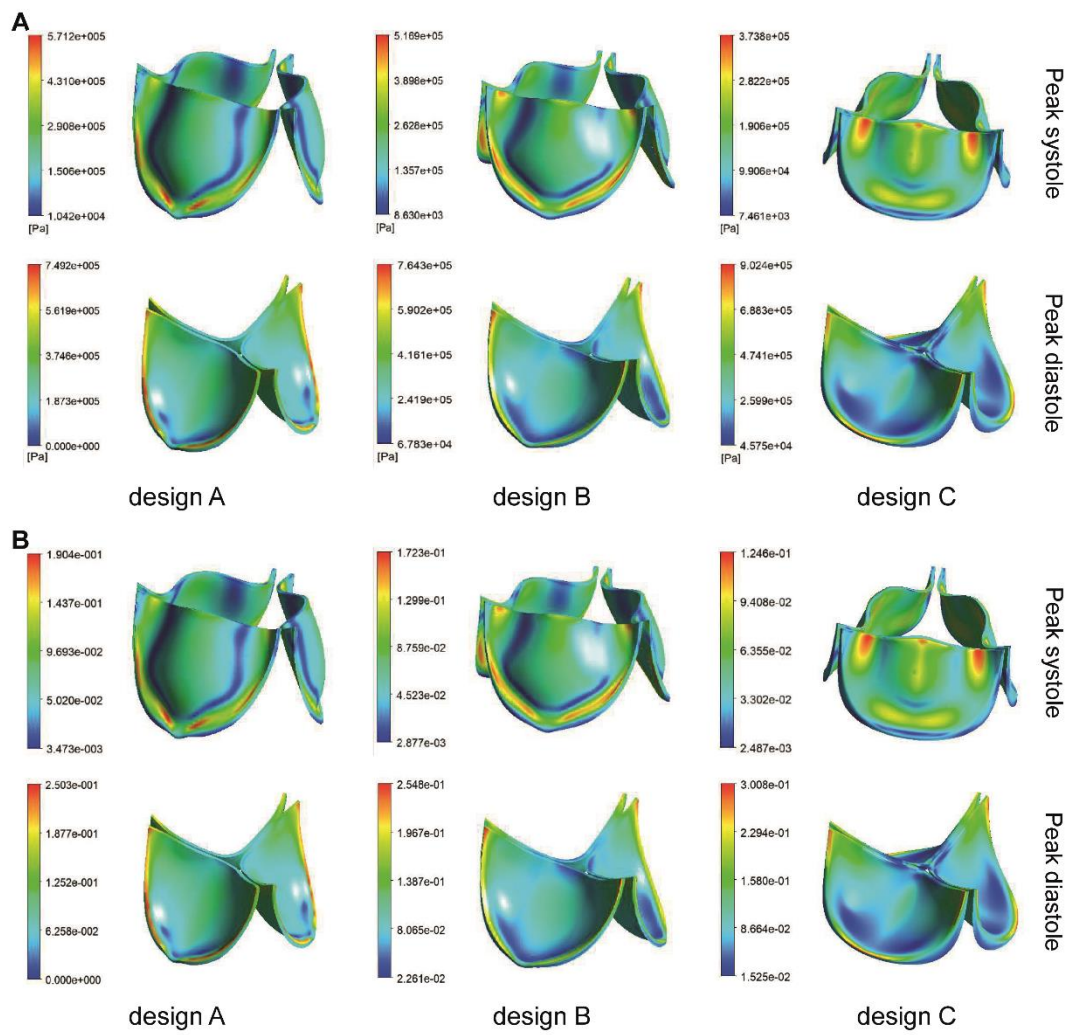
Figure S9. Stress-strain distribution on the leaflets. A) Von-Mises stress distribution at peak systole and diastole for the designs A, B and C; B) strain distribution at peak systole and diastole for the designs A, B and C.